Applied Clay Science xxx (2015) xxx–xxx

Contents lists available at ScienceDirect

Applied Clay Science

journal homepage: www.elsevier.com/locate/clay

Research paper

Structural and physicochemical aspects of drug release from layered double hydroxides and layered hydroxide salts

Ricardo Rojas [a,*], Yamila Garro Linck [b], Silvia L. Cuffini [c], Gustavo A. Monti [b,d], Carla E. Giacomelli [a]

[a] INFIQC-CONICET, Departamento de Fisicoquímica, Facultad de Ciencias Químicas, Universidad Nacional de Córdoba, Haya de la Torre s/n, 5000 Córdoba, Argentina
[b] IFEG-CONICET, 5000 Córdoba, Argentina
[c] Instituto de Ciência e Tecnologia, Universidade Federal de São Paulo, Campus São Jose dos Campos, Rua Talim, 330 (12.231-280), Villa Nair, Brazil
[d] FAMAF, Universidad Nacional de Córdoba, 5000 Córdoba, Argentina

ARTICLE INFO

Article history:
Received 10 December 2014
Received in revised form 26 February 2015
Accepted 27 February 2015
Available online xxxx

Keywords:
Layered double hydroxides
Layered hydroxide salts
Anion exchange
Ligand exchange
Charging behavior

ABSTRACT

Layered double hydroxides (LDHs) and Zn layered hydroxide salts (LHSs) present different physicochemical and interfacial properties derived from their dissimilar structure and composition, which affect the release behavior of the intercalated drug. In this work, these aspects are studied using LDHs and LHSs intercalated with ibuprofen (Ibu), naproxen (Nap) or ketoprofen (Ket) to understand the behavior of intercalation compounds as drug carriers. The structure of the solids and the interaction mode between the drugs and the layers were determined by chemical analysis, PXRD, FTIR and NMR. Further, the interfacial properties (potential zeta and hydrophilic/hydrophobic character) of the solids, as well as their drug release profiles were also comparatively studied. The drugs were attached by electrostatic interactions to LDH layers while coordinate bond was produced in the case of LHSs. The different interaction modes, together with the higher drug density between LHS layers produced more crystalline solids with larger basal spacing values than the corresponding LDH. This detailed structural study allowed for establishing the correlations between structure, interactions, morphology, interfacial properties and drug release behavior. Thus, the different interaction modes determined the surface charging behavior, while the solubility of LHS layers led to a fast drug release in neutral media. Finally, the loose drug arrangement in the hybrids caused a solubility increase in acid media. These correlations are helpful to predict and optimize the behavior of drug delivery systems based on both LDHs and Zn–LHSs.

1. Introduction

Layered double hydroxides (LDHs) and layered hydroxide salts (LHSs) are two groups of intercalation compounds with anion exchange capabilities. They hold different layer structure and bonding (Fig. 1), which leads to different physicochemical properties (Rojas and Giacomelli, 2013). LDH layer structure (Fig. 1A) is derived from that of brucite ($Mg(OH)_2$) by isomorphic substitution of divalent (M^{2+}) by trivalent (M^{3+}) ions in octahedral sites (Evans and Slade, 2006), while interlayer anions (A^{n-}) establish electrostatic interactions with the positively charged layers, the overall formula of these solids being $[M^{2+}_{1-x}M^{3+}_x(OH)_2](A^{n-})_{x/n}yH_2O$. On the other hand, LHSs present different structures with different binding modes between the interlayer anions and the layers. Thus, LHSs with formula $[Zn_5(OH)_8]A_{2/n}\cdot mH_2O$ (Fig. 1B) are derived from that of brucite by elimination of a quarter of Zn^{2+} ions in octahedral sites while additional Zn^{2+} ions are placed in tetrahedral sites at the bottom and top of each empty octahedron. Three vertices of each tetrahedron are occupied by hydroxyl anions of the layer, while the fourth is occupied by either water molecules (Arizaga et al., 2007; Biswick et al., 2009, 2012) or the interlayer anion (Poul et al., 2000; Guadalupe et al., 2008; Rojas and Giacomelli, 2013). In the first case, electrostatic interactions are mainly present between the interlayer anions and the layers while, in the latter, the anions are attached through a coordinate bond. The other layer structure ($[Zn(OH)_{2-x}]A_{x/n}$) shown in Fig. 1C, is obtained by replacing hydroxyl groups of the brucite-like structure by an oxygen atom of A^{n-}, which is attached by coordinate bond. Attaining one or another layer structure is dependent on both the synthesis conditions (Miao et al., 2006; Inoue and Fujihara, 2010) and the intercalated anion (Kongshaug and Fjellvåg, 2004).

As stated above, the differences in structure and bonding of these solids are reflected in their physicochemical and interfacial properties. Thus, exchange reactions are produced in both groups, but they are more properly described as ligand exchange reactions when anions are attached by coordinate bond (Meyn et al., 1993; Williams et al., 2012). Further, electrostatic interactions allow detachment of anions from the surface of LDH particles in aqueous dispersions, which results in positively charged particles. On the other hand, coordinate binding does not allow anion detachment from the particle surface and only ligand exchange reactions are possible when the interlayer anion is coordinated to Zn–LHS layers. Consequently, these solids present neutral or

* Corresponding author. Tel.: +54 3515353866; fax: +54 3514334188.
E-mail address: rrojas@fcq.unc.edu.ar (R. Rojas).

http://dx.doi.org/10.1016/j.clay.2015.02.030
0169-1317/

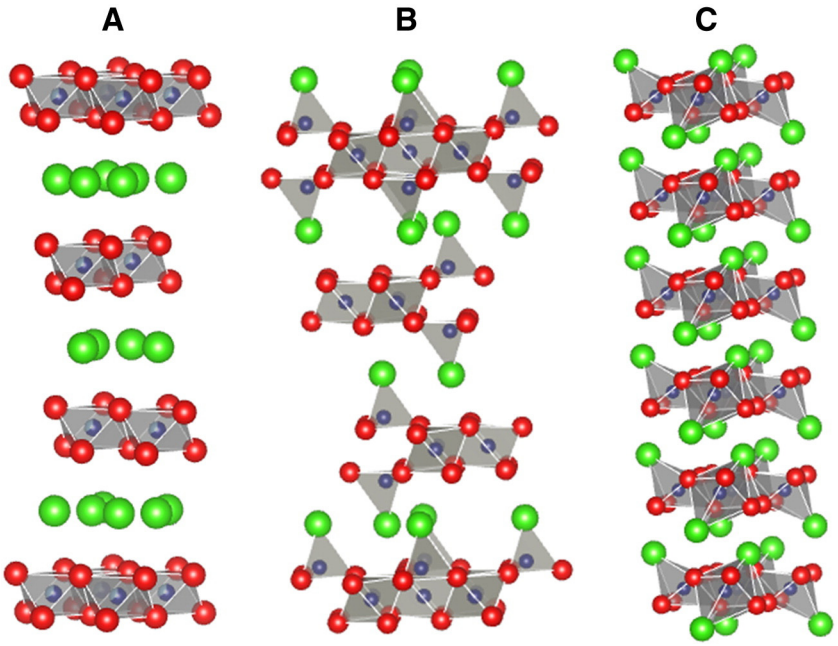

Fig. 1. Structure of LDH (A) and Zn–LHS (B and C) matrixes. Chloride was chosen as interlayer anion while water molecules were excluded from the scheme.

negatively charged particles (Rojas and Giacomelli, 2013). Finally, their dissolution behavior is different, as can be expected from the solubility of the hydroxides of the metal ions that constitute their layers (Parello et al., 2010; Rojas, 2014).

LDHs are extensively studied for pharmaceutical applications: hydrotalcite can be found in commercial antacid formulations such as Almax© and Talcid©, and they have also been proposed for the controlled release of anionic drugs due to their ease of preparation, high drug loading, release mechanism, and drug protection ability. LDHs have been intercalated with anti-inflammatory, antibiotics, antihypertensives, anticarcinogens, among others (Costantino et al., 2008; Choy et al., 2011; Rives et al., 2013, 2014; Rodrigues et al., 2013). Among these drugs, non steroidal anti-inflammatory drugs (NSAIDs) have been the most widely studied. Thus, large loadings of ibuprofen (Ibu), naproxen (Nap) or ketoprofen (Ket) have been incorporated to these solids using coprecipitation, anion exchange and reconstruction methods (Rives et al., 2013; Rojas et al., 2014). The drug content is completely released at either acid or neutral pH by matrix dissolution or anion exchange, respectively (Rojas et al., 2012) at a release rate that depends on factors such as particle size (Gunawan and Xu, 2008) and the solubility and hydrophobic character of the intercalated drug (Rojas et al., 2014). LHSS have also been intercalated with vitamins, antioxidants and NSAIDs, which are released by mechanisms similar to those of LDHs (Bull et al., 2011; Taj et al., 2013). Thus, LHSs have been intercalated with the conjugated bases of diclofenac, ibuprofen, mefenamic acid and 4-biphenylacetic acid, and formulated as tablets and enteric-coated beads (Bull et al., 2011; Richardson-Chong et al., 2012; Taj et al., 2013) in order to prevent matrix dissolution in acid media and produce modified release profiles.

Nevertheless, few comparative studies of these structurally related solids as well as their drug release behavior from LDH-drug (LDH-D) and LHS-drug (LHS-D) hybrids have been published (Yang et al., 2007). In order to explore the differences between these solids as well as the effect of the physicochemical properties of the drug, LDHs and LHSs intercalated with three NSAIDs (ibuprofen, naproxen and ketoprofen, Fig. 2) were obtained. The structure and interaction modes between the drugs and the layered matrix were determined by chemical analysis, powder X-ray diffraction (PXRD), Fourier transform infrared (FTIR) and solid state nuclear magnetic resonance (NMR) and the interfacial properties (potential zeta and hydrophilic/hydrophobic character) of the hybrids, as well as the drug release profiles were comparatively studied.

2. Materials and methods

Ibu, Ket and Nap anhydrous acids (≥98% purity, Parapharm®, Buenos Aires, Argentina), $MgCl_2 \cdot 6H_2O$ (Baker), $AlCl_3 \cdot 6H_2O$ (Anedra), $ZnCl_2$ (Cicarelli), NaOH (Baker), NH_4OH (Merck) and deionized water

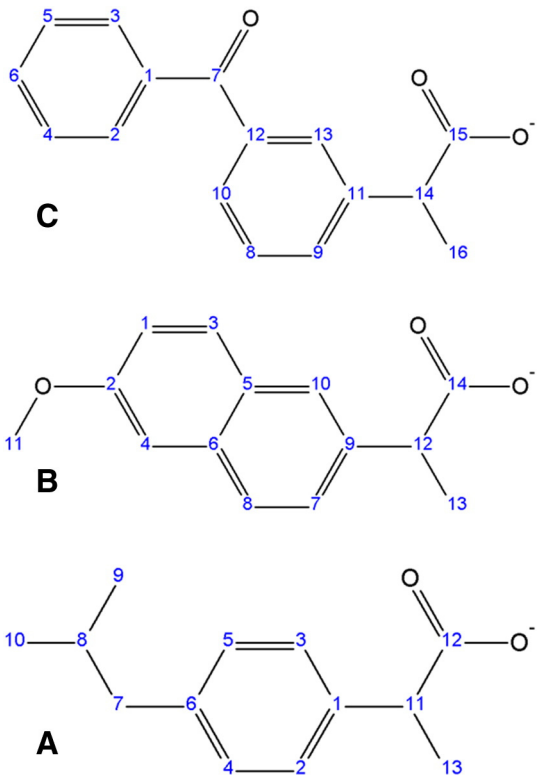

Fig. 2. Structural formulae of the intercalated drugs: A) ibuprofen, B) naproxen, C) ketoprofen.

Please cite this article as: Rojas, R., et al., Structural and physicochemical aspects of drug release from layered double hydroxides and layered hydroxide salts, Appl. Clay Sci. (2015), http://dx.doi.org/10.1016/j.clay.2015.02.030

(Milli-Q system, 18.2 MΩ), were used in the experiments, which were carried out at room temperature (25 °C) unless otherwise stated.

2.1. Synthesis

Both LDH-D and LHS-D hybrids (containing either Ibu, Nap or Ket) were synthesized by the coprecipitation method at constant pH (He et al., 2006; Arizaga et al., 2007; Rojas et al., 2012; Rojas and Giacomelli, 2013). A 0.1 L solution containing the metal ions (0.04 mol $AlCl_3$; 0.12 mol $MgCl_2$) was added drop wise to a 0.1 L solution containing 0.06 mol of the corresponding drug (1.5 times excess against the $AlCl_3$ amount) under vigorous stirring at pH = 9, controlled by addition of a 2 mol L^{-1} NaOH solution. The obtained slurries were centrifuged, washed and finally dried at 50 °C until constant weight. The hybrids were named LDH-Ibu, LDH-Ket and LDH-Nap according to the intercalated drug. For LHSs, the metal ion solution (0.06 mol $ZnCl_2$ in 200 mL H_2O) was added to a 200 mL solution of the corresponding drug (0.036 mol) and pH was set to 7 by addition of 1 mol L^{-1} NH_4OH solution. The obtained slurries were aged overnight and then centrifuged, washed and dried as previously described. The hybrids were denoted as LHS-Ibu, LHS-Ket, and LHS-Nap.

2.2. Structural characterization

Mg and Al contents were determined by atomic absorption spectrometry in a Varian AA240 instrument. The samples were dissolved in HNO_3 and afterwards diluted to meet the calibration range. C content was determined using a CHN 2400 Series II Elemental Analyzer, using cysteine as reference. Water content was estimated by thermogravimetric analysis between 25 and 200 °C, carried out in a SETARAM Setsys Evolution 16/18 instrument at a 5 °C min^{-1} heating rate (Supplementary material, Fig. S1). PXRD patterns were recorded with a Phillips X'pert Pro instrument using a CuKα lamp (λ = 1.5408 Å) at 40 kV and 40 mA between 3° and 60° (2θ) in step mode (0.05°, 1.2 s). FTIR spectra were measured with a FTIR Bruker IFS28 instrument using KBr pellets (1:100 sample:KBr ratio). High resolution solid state ^{13}C cross polarization/magic angle spinning (CP/MAS) NMR experiments were performed on a Bruker Avance II-300 spectrometer (Larmor frequency of 300.13 MHz and 75.46 MHz for ^{1}H and ^{13}C respectively) equipped with a 4 mm MAS probe. All samples were spun at 10 kHz. The ^{13}C CP/MAS spectra were recorded using variable amplitude ramped CP pulse (Harris, 1994) of 2 ms. TPPM sequence was used for the heteronuclear decoupling during acquisition with a proton field H_{1H} satisfying $\omega_{1H}/2\pi = \gamma_H H_{1H} = 60$ kHz (Bennett et al., 1995). The recycling delay was 4 s. The quaternary carbon edition experiments (Non Quaternary Suppression, NQS) were performed on all the samples (Harris, 1994). These experiments allowed us to identify quaternary carbon signals and methyl groups helping in the accurate assignment of the signals. The assignments of the signals for the pure drugs were done by comparing to the chemical shift measured with the molecules in solution using ACD Labs NMR Predictor program and taking into account the NQS experiment, while the assignments for the hybrids were performed by comparing the chemical shifts to those of the pure drug. The complete atomic numbering for the assignments is included in Fig. 2.

2.3. Interfacial and morphological characterization

The hydrodynamic apparent diameter (d) and zeta potential (ζ) of the samples were determined by dynamic light scattering (DLS) and electrophoretic light scattering (ELS) measurements, respectively, using a Delsa Nano C instrument (Beckman Coulter). Aqueous dispersions of the hybrids (0.1 g L^{-1} in $5\cdot10^{-2}$ mol L^{-1} NaCl) were prepared and sonicated for 30 min. ζ values were determined at different pH values, adjusted by addition of a NaOH solution. d and polydispersity values at pH = 9 were calculated from the autocorrelation function ($g^{(2)}$) using the cumulants method, while electrophoretic mobilities were converted to ζ using the Smoluchowski equation. Contact angle (CA) measurements were performed by the sessile drop method using a homemade goniometer and deionized water drops over tablets of the corresponding hybrids prepared at 2 tons with an 11 mm die. Scanning electron microscopy (SEM) images were obtained with a FE-SEM Σigma instrument on samples covered with a Cr layer.

2.4. Drug release kinetics

United States Pharmacopoeia (USP) simulated intestinal (SIF, 0.05 mol L^{-1} phosphate buffer pH = 6.8 ± 0.1) and simulated gastric (SGF, HCl pH = 1.2 ± 0.1 in 0.05 mol L^{-1} NaCl) fluids without enzymes was selected as release media. Drug release from particulate LDH-D and LHS-D hybrids was studied in 0.05 L propylene tubes (triplicate experiments) that were continuously shaken in an orbital agitator (60 rpm) at room temperature. An accurately weighted amount of particulate hybrid, adjusted to contain 0.030 g of drug in all cases, was dispersed in 0.030 L of release medium. At defined time intervals, samples were withdrawn and filtered, and the drug concentration ([D]) was determined by UV–vis spectroscopy (Shimadzu UV1601 instrument). The percentage of dissolved drug (%D) was calculated as $\%D = [D] / [D]_{max}$, where $[D]_{max}$ is the maximum [D] (1 g/L). The solubility of the pure drugs in SGF was determined in 0.030 L dispersions containing 0.030 g of the corresponding drug.

The drug release data were analyzed using two usual mathematical models (Costa and Sousa Lobo, 2001): Higuchi (Eq. (1)), associated with diffusion as the rate determining step of the process, and zero order (Eq. (2)) related to surface reaction controlled kinetics:

$$\%D = kt^{1/2} \quad (1)$$

$$\%D = kt \quad (2)$$

where $\%D$ is the percentage of dissolved drug at time t and k is the kinetic release constant.

3. Results and discussion

3.1. Structural characterization

The chemical analyses of the samples and their theoretical chemical formulae are included in Table 1. The layers of LDH-D hybrids showed similar composition ($[Mg_{1-x}Al_x(OH)_2]^{x+}$, $x = 0.29$). The Mg/Al ratio of the samples was lower than that of the starting solution of the synthesis, indicating a partial dissolution of Mg^{2+} ions during the solid washing (Jobbágy and Regazzoni, 2011). The D^-/Al^{3+} ratio was near 1 in all cases, indicating that charge of the layers was completely compensated for by the corresponding drug. Moreover, LDH-Ibu showed a drug excess, which, according to previous works (Rojas et al., 2012), was produced by incorporation of the anionic drug at the particle surface. The incorporation of the anion excess was explained by hydrophobic interactions of the apolar section of the drug, which allowed for overcoming the electrostatic repulsions produced once the layer charge is completely compensated for. On the other hand, LHS-D hybrids exhibited different OH/Zn ratios, which indicated that different structures were obtained: $[Zn_5(OH)_8]A_{2/n}\cdot mH_2O$ (Fig. 1B) for LHS-Ibu and $[Zn(OH)_{2-x}]A_x\cdot mH_2O$ (Fig. 1C) for LHS-Nap and LHS-Ket. A drug excess was obtained for LHS-Ibu while, for LHS-Nap and LHS-Ket, its presence could not be determined due to the non-stoichiometric OH/Zn ratio.

The PXRD pattern of each sample (Fig. 3) was indexed with a single set of cell parameters. The PXRD patterns of LDH-D hybrids were indexed in a rhombohedral unit cell and displayed well developed peaks at 2θ below 30°, corresponding to 00 l reflections that led to similar basal spacing values (22.0–22.2 Å). These values were in good

Please cite this article as: Rojas, R., et al., Structural and physicochemical aspects of drug release from layered double hydroxides and layered hydroxide salts, Appl. Clay Sci. (2015), http://dx.doi.org/10.1016/j.clay.2015.02.030

Table 1
Chemical composition and formula, cell parameters, contact angle (*CA*) and residual weight loss upon calcination at 1000 °C of the LDH-D and LHS-D hybrids.

Sample	% Mg	% Al	% Zn	% C	% H_2O	Chemical formula	*CA* (°)	% W_e[a]	% W_c[b]
LDH-Ibu	11.0	5.2	–	37.2	9.5	$Mg_{0.71}Al_{0.29}(OH)_2Ibu_{0.35}\cdot 0.77\ H_2O$	86	70.3	70.1
LDH-Ket	10.5	4.9	–	36.7	8.4	$Mg_{0.71}Al_{0.29}(OH)_2Ket_{0.26}\cdot 0.65\ H_2O$	65	69.5	68.5
LDH-Nap	11.9	5.3	–	34.9	9.3	$Mg_{0.71}Al_{0.29}(OH)_2Nap_{0.29}\cdot 0.71\ H_2O$	72	68.6	68.6
LHS-Ibu	–	–	32.5	36.7	4.2	$Zn_5(OH)_8Ibu_{2.4}\cdot 2.2\ H_2O$	85	57.3	59.1
LHS-Ket	–	–	28.7	46.3	4.4	$Zn(OH)_{1.4}Ket_{0.6}\cdot 0.6\ H_2O$	65	68.6	67.8
LHS-Nap	–	–	23.6	45.6	4.0	$Zn(OH)_{1.2}Nap_{0.8}\cdot 0.9\ H_2O$	87	71.8	71.5

[a] % W_e, residual weight percentage at 1000 °C (experimental).
[b] % W_c, residual weight percentage at 1000 °C (calculated from the chemical formula).

accord with those reported by other authors for LDH-D hybrids with Ibu (Ambrogi et al., 2001; Costantino et al., 2008; Rojas et al., 2012), Nap (del Arco et al., 2009; Carriazo et al., 2010) and Ket (Ambrogi et al., 2003; San Román et al., 2012). In those works, the basal spacing values obtained were assumed to be due to a drug arrangement in a tilted bilayer disposition (Berber et al., 2008; Carriazo et al., 2010), as the size of the molecules (between 9 and 11 Å) was less than the distance between the layers, calculated by substraction of the layer thickness (4.8 Å) to the basal spacing.

The patterns of LHS-D hybrids showed narrower peaks than those of LDH in all the measured ranges, indicating high ordering of the solids. The pattern of LHS-Ibu was different from those of the LHS-Nap and LHS-Ket ones, which confirmed the different layer structure of these LHS-D hybrids. LHS-Ibu pattern was indexed in a hexagonal cell unit, typical of solids with $[Zn_5(OH)_8]A_2$ layers like simonkolleite ($[Zn_5(OH)_8]Cl_2\cdot nH_2O$, JCPDS card 07-0155). Its basal spacing, calculated from the (00 l) reflections, was 26.5 Å. On the other hand, LHS-Nap and LHS-Ket patterns were indexed in a monoclinic unit cell, as expected from the composition of these solids. The structure of $[Zn(OH)_{2-x}]A_{x/n}$ layers were similar to that of zinc hydroxide nitrate ($Zn_3(OH)_4(NO_3)_2$, JCPDS card 70-1361), and zinc hydroxide terephtalate ($Zn_3(OH)_4(tp)_2$) (Carton et al., 2006). The basal spacing values obtained (23.6 Å and 22.9 Å for LHS-Nap and LHS-Ket, respectively) were higher than those of the corresponding LDHs. This basal spacing increase was attributed to the higher binding site density of LHS layers compared to LDH ones (Arizaga et al., 2007; Rojas and Giacomelli, 2013), which led to a more compact and less tilted disposition of the anions in the interlayer of the former (Yang et al., 2007).

The FTIR spectra of the samples (Fig. 4) presented bands assigned to υ_{asym} (between 1552 and 1581 cm^{-1}) and υ_{sym} (between 1390 and 1412 cm^{-1}) of the carboxylate groups of the drugs as well as bands at 1448–1464 cm^{-1} and 1352–1365 cm^{-1} due to $\delta(CH_2)$. The difference between the maximum of the asymmetric and symmetric vibration bands of carboxylate groups ($\Delta\upsilon = \upsilon_{asym} - \upsilon_{asym}$) is considered as indicative of the type of interactions between the carboxylate group and the layers (Wypych et al., 2005). Thus, $\Delta\upsilon$ for LDHs (between 150 and 164 cm^{-1}) is lower than for LHSs (between 166 and 185 cm^{-1}). This result indicated that the drugs presented non-directional, electrostatic interactions with LDH layers, while a coordinate bond was established by the carboxylate group of the drug with Zn^{2+} ions of LHS layers. The spectra also portrayed bands representative of each anion: a band at 1655 and 1658 cm^{-1} corresponding to the ketone group was observed in the case of LDH-Ket and LHS-Ket, respectively (Ambrogi et al., 2003). On the other hand, ν(C–O) and ν(C–O–C) bands of the ether group were registered at 1267–1263 cm^{-1} and 1161 cm^{-1}, respectively, for the Nap containing samples (del Arco et al., 2004). None of the hybrids displayed bands at 1700–1750 cm^{-1} (ν(COOH)), which indicated the absence of the drug acid form in the LDH-D hybrids (Nakamoto, 1997). This also

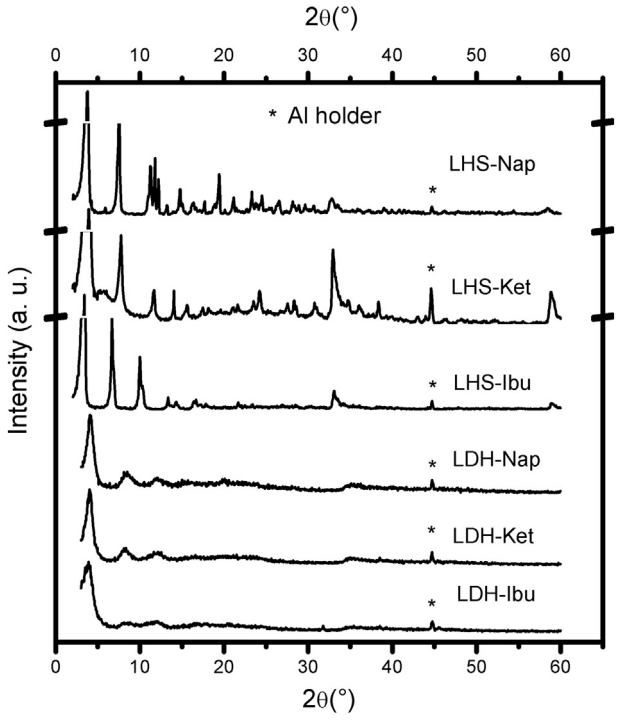

Fig. 3. PXRD patterns of LDH-D and LHS-D hybrids.

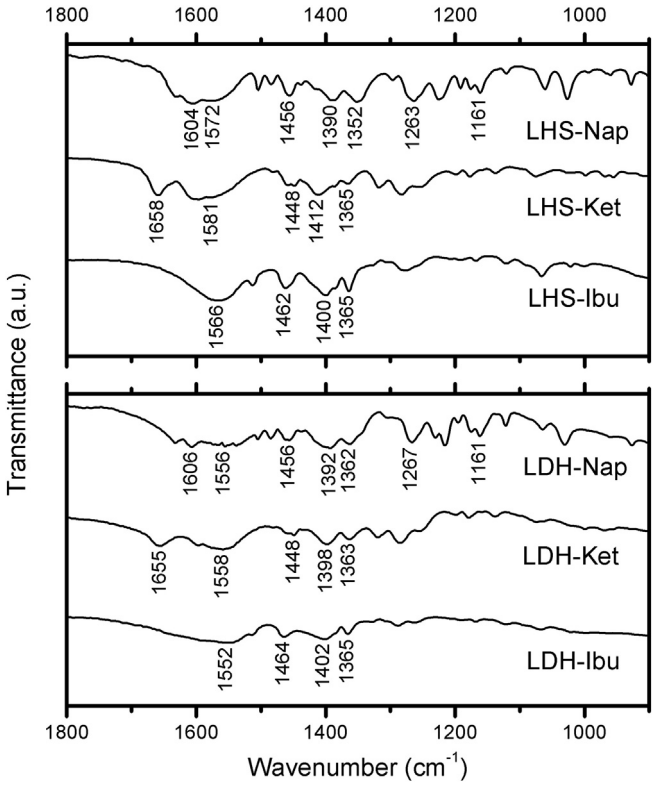

Fig. 4. FTIR spectra of LDH-D and LHS-D hybrids.

confirmed that the acid form was not co-intercalated between the layers, the drug excess being exclusively placed as anions at the particle surface.

The ^{13}C NMR spectra (Fig. 5) indicated that the drug molecular structure is preserved upon intercalation but the position and width of the peaks are slightly changed, indicating that the drug arrangement is different from that of the pure drug (Mohanambe and Vasudevan, 2005). These changes allowed for determining the interactions between the drugs and the layers as well as the degree of drug disorder in the hybrids compared to that in the pure drug. Thus, the ^{13}C spectra for LDH-Ibu and LHS-Ibu showed broader resonances than that of pure Ibu, which denoted a higher disorder when the drug was confined between the layers. Due to the bilayer arrangement of the anions, the anions interacted with the layers at both ends. As a consequence, the main differences with the pure drug were expected for these sections (del Arco et al., 2004), while the middle aromatic part only was expected to be affected exclusively by the disorder increment. Nevertheless, the δ_{13C} values for carboxylate carbon (C12) and the neighboring carbons (C11 and C13) were similar to that of the pure drug, which indicated that the interactions between the layers and the drug were similar to that with protons in the pure drug. On the other hand, the δ_{13C} variations for C8, C9 and C10 were indicative of a change to a less hydrophobic environment of the isopropyl group of the drug in the hybrids.

Compared to Ibu, a larger disorder increase was produced by Ket intercalation between LDH and LHS layers. On the one hand, δ_{13C} values of the carboxylate carbon (C15) were lower for the intercalated drug than for pure Ket, which indicated a weaker interaction with the layers. On the other hand, the shift to higher δ_{13C} values of the ketone carbon (C7) was indicative of an interaction between this group and the layer, probably the opposite, considering the spatial disposition of carboxylate and ketone groups.

Finally, a negligible resonance broadening was produced when Nap was confined in LDH-Nap and LHS-Nap hybrids, which indicated a more ordered arrangement of the drug molecules between the layers in these hybrids. Moreover, Nap signals were split in the hybrids, indicating that Nap anions were placed in two different, well defined environments. The δ_{13C} values of the carboxylate carbon (C14) were higher than for the pure drug, which indicated that strong interactions between Nap

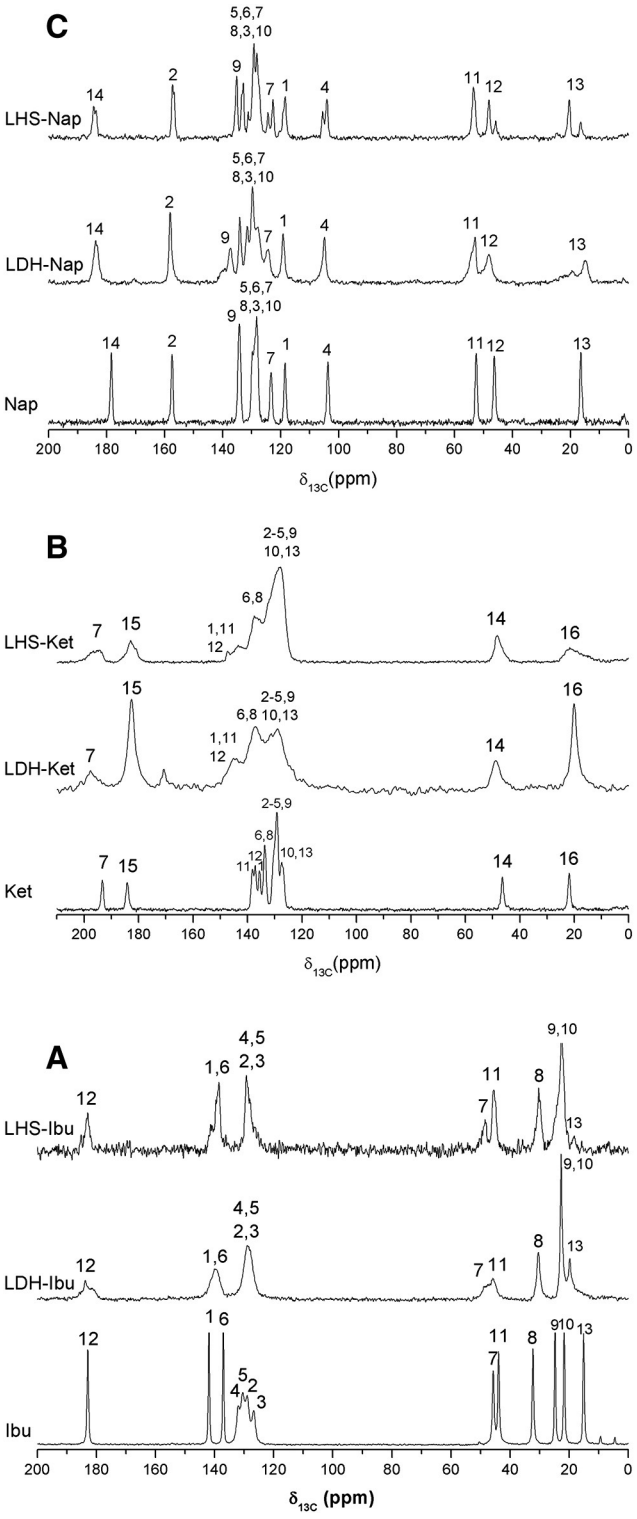

Fig. 5. NMR spectra of the LDH-D and LHS-D hybrids with ibuprofen (A), naproxen (B) and ketoprofen (C). Spectra of pure drugs are also given as reference. The included numbers indicate the position of the C atoms (see Fig. 2).

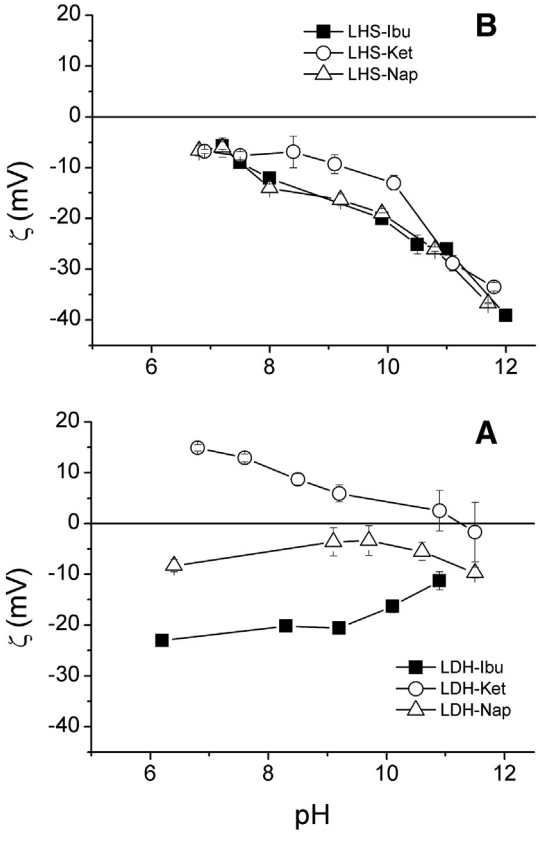

Fig. 6. ζ vs. pH curves of LDH-D (A) and LHS-D (B) hybrids with ibuprofen, naproxen and ketoprofen.

Please cite this article as: Rojas, R., et al., Structural and physicochemical aspects of drug release from layered double hydroxides and layered hydroxide salts, Appl. Clay Sci. (2015), http://dx.doi.org/10.1016/j.clay.2015.02.030

anions and the layers were produced. This strong interaction caused the higher ordering of the drug between the layers of the hybrid.

The TGA and DTA profiles of both LDHs and LHSs (Supporting information, Fig. S1) were interpreted on the basis of three main processes: interlayer water loss, dehydroxylation of the layers and drug degradation. The main difference between the profiles of LDHs and LHSs was the temperature range where the dehydroxylation process was produced. For LDHs, dehydroxylation was produced at $T > 200$ °C, overlapped with the interlayer anion loss step while, it was produced at $T < 200$ °C for LHSs, separated from dehydroxylation step and near to the interlayer water loss one. The experimental residual weight of the solids at 1000 °C was in good accord with that calculated from the chemical formula proposed considering that only the metal oxides remained at this temperature (Table 1).

3.2. Interfacial and morphological characterization

The ζ vs. pH curves (Fig. 6) exhibited different profiles depending on the solid structure. As already reported (Rojas et al., 2014), the ζ profile of LDH-D hybrids was strongly dependent on the intercalated anion: LDH-Ibu particles were negatively charged in the whole pH range measured, while LDH-Ket present positive ζ values up to pH = 11 approximately. This result indicated that, while Ket^- anions were exclusively bonded to the inorganic matrix by electrostatic interactions, hydrophobic interactions are also concurrent in the case of Ibu^- anions (Hansch et al., 1995). On the other hand, all LHS hybrids particles portrayed slightly negative ζ values at pH = 8, similarly to that obtained for chlorobenzoate and chlorobenzylsulfonate intercalated Zn–LHSs (Rojas and Giacomelli, 2013). The charging behavior of Zn–LHS hybrids was explained by the coordinate bond of the drugs to Zn^{2+} ions, which caused a complete screening of the layer charge both in the bulk and on the particle surface. As pH decreases, the absolute value of ζ increased in all cases, which was assigned to deprotonation of hydroxyl groups of the hybrid surface (Rojas et al., 2010; Rojas and Giacomelli, 2013). On the other hand, the hydrophobic/hydrophilic character of the solids was mainly determined by the interlayer anion. Thus, LDH-D and LHS-D hybrids intercalated with the same drug exhibited similar contact angle values (Table 1). Only Nap containing hybrids exhibited a different behavior, which was assigned to the ordered arrangement in these hybrids (see NMR spectra discussion). Only LHS-Nap exhibited a different CA than LDH-Nap, which was assigned to the much denser arrangement of the drug on the surface of the LHS particles.

The particle size and shape of LDH-D and LHS-D hybrids were assessed by DLS determinations and SEM images. According to DLS measurements, both LDH-D and LHS-D hybrids presented large *d* (around 6–10 μm) and high polydispersity in aqueous solution (data not shown). On the other hand, the SEM images showed the different morphology of LDH and LHS particles. LDH particles were formed by agglomeration of smaller units or platelets of around 300 nm (Fig. 7). These platelets presented high diameter to thickness ratio and irregular

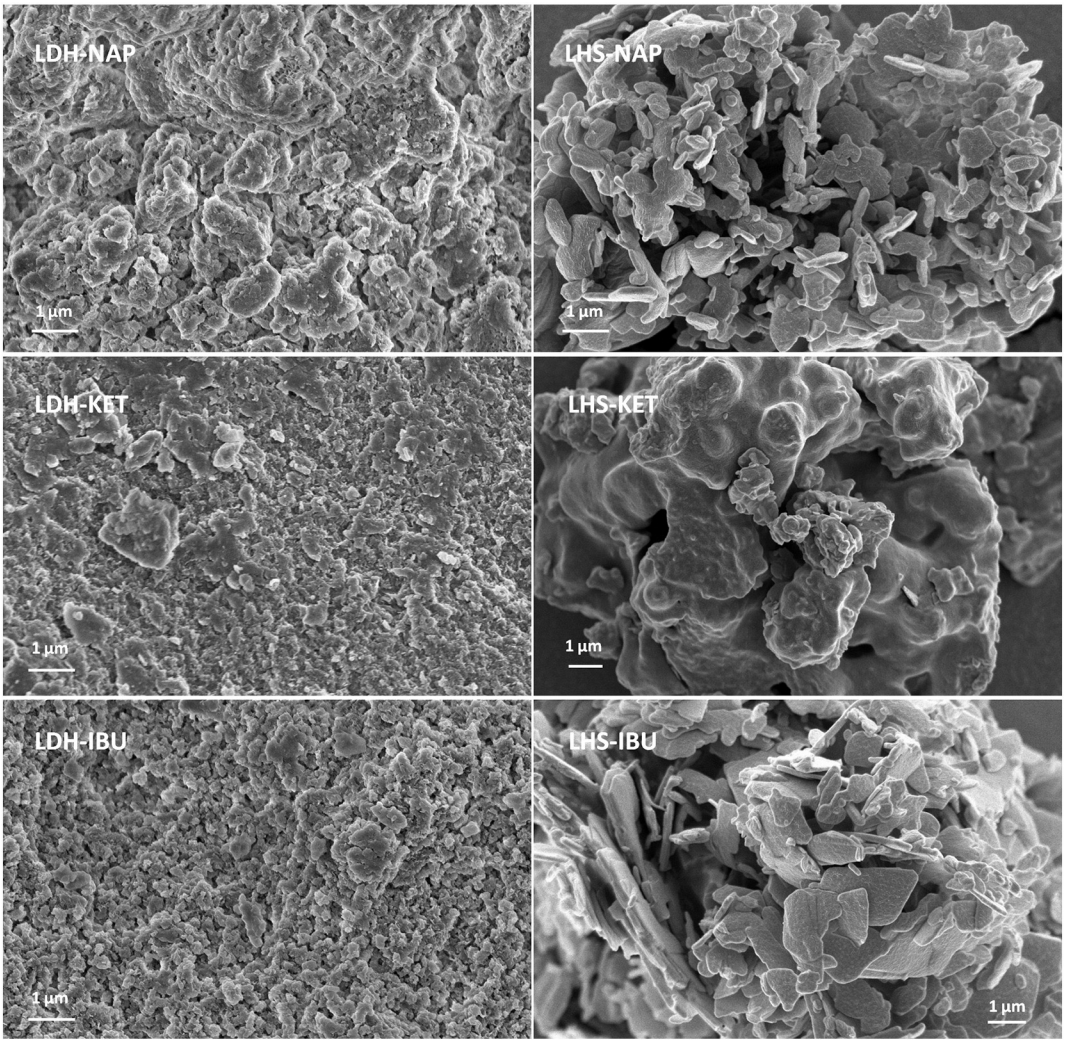

Fig. 7. SEM images of LDH-D and LHS-D hybrids with ibuprofen, naproxen and ketoprofen.

Please cite this article as: Rojas, R., et al., Structural and physicochemical aspects of drug release from layered double hydroxides and layered hydroxide salts, Appl. Clay Sci. (2015), http://dx.doi.org/10.1016/j.clay.2015.02.030

shape (Zhang and Evans, 2012; Rojas et al., 2014). LHS-D particles were also formed by agglomeration of larger platelets with a more regular shape and a less compact disposition than LDH-D platelets. Only LHS-Ket portrayed a smooth surface indicating a compact disposition of its platelets.

3.3. Drug release kinetics

The drug release behavior (Fig. 8) was affected by the different characteristics of LDHs and LHSs as well as by the physicochemical properties of the intercalated drug. Drug release in SIF (Fig. 8A and B) was slower from LDH than from LHS hybrids. A complete release of the drug content was reached at approximately 240 and 120 min in each case. A burst release was registered in all cases, but it was more significant for LHSs (60–80%D) than for LDHs (20–40%D). According to previous works (Parello et al., 2010; Rojas et al., 2012), Mg–Al LDHs are massively dissolved at pH values lower than 5, while at higher pH values only selective, partial dissolution of Mg^{2+} ions is produced. On the other hand, LHS dissolution starts at pH values higher than 7 (Rojas and Giacomelli, 2013). Hence, the first, fast step was assigned to the dissolution process of either LDH or LHS matrixes, as %D produced was consistent with the different solubility of the matrixes. Matrix dissolution was then the main release mechanism in the case of LHS-D hybrids, although the occurrence of anion exchange processes cannot be discarded. On the other hand, the best fits of LDH-D profiles were obtained with the Higuchi equation (Supplementary material, Table S1), which indicated that the main release mechanism was anion exchange. The similar profile for all LDH-D hybrids was indicative of the high affinity for LDH layers of phosphate anions, which induced a fast and complete release independently of the drug.

The %D vs. t profiles in SGF (Fig. 8C and D) were mostly dependent on the intercalated drug. Both LDH and LHS layers were fully dissolved in SGF, the drug content being released to the media shortly after the hybrid dispersion (Parello et al., 2010; Bull et al., 2011). Nevertheless, the drug loading was not completely dissolved due to the low solubility of the drugs in SGF. The final drug concentration was controlled by the solubility of the drug, which increased in the order Nap < Ibu < Ket. Nevertheless, $\%D_{240}$ was higher than that obtained for the pure drug in experiments at the same conditions (2.7, 1.5 and 9.2 for Ibu, Nap and Ket, respectively). The higher solubility of NSAIDs when intercalated in the LDH matrix has been reported by other authors (Berber et al., 2008; del Arco et al., 2010; Rojas et al., 2012) and assigned to the anionic form and confined arrangement of the drug between the layers of the inorganic matrixes. This assumption correlated well with the NMR spectra, which pointed to a disordered arrangement of the anions in the interlayer of LDH-D and LHS-D hybrids. For LHS-Ibu, LDH-Nap and LHS-Nap, the drug dissolution was so fast and/or so small that it prevented fitting the kinetic profile. However, the remaining datasets were best fitted with the zero order model, which indicated that a surface reaction was controlling the kinetics of drug dissolution. In a previous work (Rojas et al., 2012), this surface reaction was assigned to the dissolution of the acid drug from the surface of particles of either the pure drug or the hybrids. The effect of the layer structure in the release profiles was more subtle than in SIF. However, the dissolution profile from LHS-Ibu was quite different from those of LHS-Nap and LHS-Ket, which was related to the different layer structure of the former.

4. Conclusions

NSAID hybrids with Mg–Al layered double hydroxides (LDH-D) and Zn layered hydroxide (LHS-D) can be easily obtained by a coprecipitation method at constant pH. The obtained hybrids differed in their structure and interaction modes between the drug and the layers. The different interaction modes, together with the higher drug density between LHS layers produced more crystalline solids with larger basal spacing values than the corresponding LDHs. The differences in structure, interactions and composition were essential to explain the interfacial properties and drug release behaviors of LDH-D and LHS-D hybrids. Thus, the different interaction modes determined the surface charging behavior, while the solubility of LHS layers led to a fast drug release in neutral media. Finally, the loose drug arrangement in the hybrids caused a solubility increase in acid media. These correlations are helpful to predict and optimize the behavior of drug delivery systems based on both LDHs and Zn–LHSs.

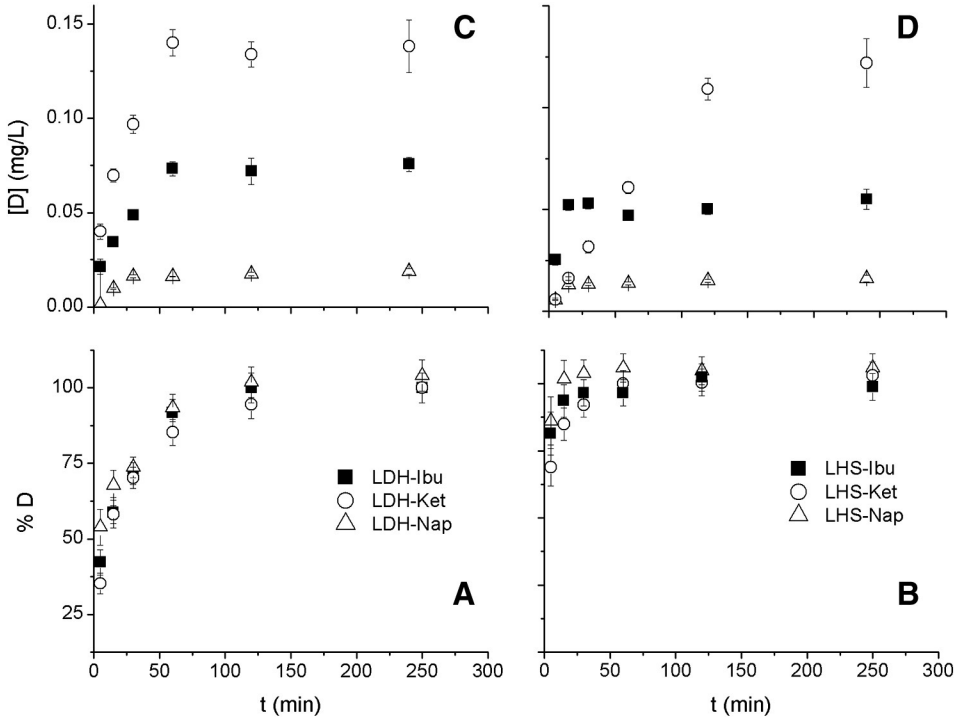

Fig. 8. Release profiles of LDH-D (A and C) and LHS-D (B and D) hybrids in SIF (A and B) and SGF (C and D).

Please cite this article as: Rojas, R., et al., Structural and physicochemical aspects of drug release from layered double hydroxides and layered hydroxide salts, Appl. Clay Sci. (2015), http://dx.doi.org/10.1016/j.clay.2015.02.030

Acknowledgements

Financial support by SeCyT-UNC project number 05/C585, FONCyT, project numbers 12/0634, 10/2116 and 10/1096, and CONICET, PIP 11220120100575 and 11220090100754, are gratefully acknowledged.

Appendix A. Supplementary data

The following files are available free of charge: a word document containing, Fig. S1: Thermal analysis of the hybrids and Tables S1 and S2, kinetic constant obtained with the Higuchi model for release profiles in SIF media and with zero order model for release profiles in SGF, respectively. Supplementary data associated with this article can be found, in the online version, at http://dx.doi.org/10.1016/j.clay.2015.02.030.

References

Ambrogi, V., Fardella, G., Grandolini, G., Perioli, L., 2001. Intercalation compounds of hydrotalcite-like anionic clays with antiinflammatory agents—I. Intercalation and in vitro release of ibuprofen. Int. J. Pharm. 220, 23–32.

Ambrogi, V., Fardella, G., Grandolini, G., Nocchetti, M., Perioli, L., 2003. Effect of hydrotalcite-like compounds on the aqueous solubility of some poorly water-soluble drugs. J. Pharm. Sci. 92, 1407–1418. http://dx.doi.org/10.1002/jps.10411.

Arizaga, G., Satyanarayana, K., Wypych, F., 2007. Layered hydroxide salts: synthesis, properties and potential applications. Solid State Ionics 178, 1143–1162. http://dx.doi.org/10.1016/j.ssi.2007.04.016.

Bennett, A.E., Rienstra, C.M., Auger, M., Lakshmi, K.V., Griffin, R.G., 1995. Heteronuclear decoupling in rotating solids. J. Chem. Phys. 103, 6951. http://dx.doi.org/10.1063/1.470372.

Berber, M.R., Minagawa, K., Katoh, M., Mori, T., Tanaka, M., 2008. Nanocomposites of 2-arylpropionic acid drugs based on Mg–Al layered double hydroxide for dissolution enhancement. Eur. J. Pharm. Sci. 35, 354–360. http://dx.doi.org/10.1016/j.ejps.2008.08.006.

Biswick, T., Jones, W., Pacuła, A., Serwicka, E., Podobinski, J., 2009. Evidence for the formation of anhydrous zinc acetate and acetic anhydride during the thermal degradation of zinc hydroxy acetate, Zn5(OH)8(CH3CO2)2·4H2O to ZnO. Solid State Sci. 11, 330–335. http://dx.doi.org/10.1016/j.solidstatesciences.2008.06.018.

Biswick, T., Park, D.-H., Choy, J.-H., 2012. Enhancing the UV A1 screening ability of caffeic acid by encapsulation in layered basic zinc hydroxide matrix. J. Phys. Chem. Solids 73, 1510–1513. http://dx.doi.org/10.1016/j.jpcs.2011.11.039.

Bull, R.M.R., Markland, C., Williams, G.R., O'Hare, D., 2011. Hydroxy double salts as versatile storage and delivery matrices. J. Mater. Chem. 21, 1822. http://dx.doi.org/10.1039/c0jm03020a.

Carriazo, D., del Arco, M., Martín, C., Ramos, C., Rives, V., 2010. Influence of the inorganic matrix nature on the sustained release of naproxen. Microporous Mesoporous Mater. 130, 229–238. http://dx.doi.org/10.1016/j.micromeso.2009.11.014.

Carton, A., Abdelouhab, S., Renaudin, G., Rabu, P., François, M., 2006. Structure of zinc hydroxy-terephthalate: Zn3(OH)4(C8H4O4). Solid State Sci. 8, 958–963. http://dx.doi.org/10.1016/j.solidstatesciences.2006.02.043.

Choy, J.H., Oh, J.M., Choi, S.J., 2011. Layered double hydroxides as controlled release materials. In: Ducheyne, P. (Ed.), Comprehensive Biomaterials. Elsevier, Oxford, pp. 545–557. http://dx.doi.org/10.1016/B978-0-08-055294-1.00142-2.

Costa, P., Sousa Lobo, J.M., 2001. Modeling and comparison of dissolution profiles. Eur. J. Pharm. Sci. 13, 123–133. http://dx.doi.org/10.1016/S0928-0987(01)00095-1.

Costantino, U., Ambrogi, V., Nocchetti, M., Perioli, L., 2008. Hydrotalcite-like compounds: versatile layered hosts of molecular anions with biological activity. Microporous Mesoporous Mater. 107, 149–160. http://dx.doi.org/10.1016/j.micromeso.2007.02.005.

Del Arco, M., Gutiérrez, S., Martín, C., Rives, V., Rocha, J., 2004. Synthesis and characterization of layered double hydroxides (LDH) intercalated with non-steroidal anti-inflammatory drugs (NSAID). J. Solid State Chem. 177, 3954–3962. http://dx.doi.org/10.1016/j.jssc.2004.08.006.

Del Arco, M., Fernandez, A., Martin, C., Rives, V., 2009. Release studies of different NSAIDs encapsulated in Mg,Al,Fe-hydrotalcites. Appl. Clay Sci. 42, 538–544. http://dx.doi.org/10.1016/j.clay.2008.06.014.

Del Arco, M., Fernández, A., Martín, C., Rives, V., 2010. Solubility and release of fenbufen intercalated in Mg, Al and Mg, Al, Fe layered double hydroxides (LDH): the effect of Eudragit® S 100 covering. J. Solid State Chem. 183, 3002–3009. http://dx.doi.org/10.1016/j.jssc.2010.10.017.

Evans, D.G., Slade, R.T.C., 2006. Structural aspects of layered double hydroxides. In: Duan, X., Evans, D.G. (Eds.), Layered Double Hydroxides, pp. 1–87.

Guadalupe, G., Arizaga, C., Salvio, A., Eduardo, J., Gardolinski, C., Wypych, F., 2008. Chemical modification of zinc hydroxide nitrate and Zn–Al-layered double hydroxide with dicarboxylic acids. 320, 168–176. http://dx.doi.org/10.1016/j.jcis.2007.12.038.

Gunawan, P., Xu, R., 2008. Direct control of drug release behavior from layered double hydroxides through particle interactions. J. Pharm. Sci. 97, 4367–4378.

Hansch, C., Leo, A., Hoekman, D., 1995. Exploring QSAR: hydrophobic, electronic and steric constants. ACS Professional Reference Book. American Chemical Society, Washington DC.

Harris, R.K., 1994. Nuclear Magnetic Resonance Spectroscopy. Longman Scientific and Technical, London, UK.

He, J., Wei, M., Kang, Y.-G., Evans, D.G., Duan, X., 2006. Preparation of layered double hydroxides. In: Evans, D.G., Duan, X. (Eds.), Layered Double Hydroxides. Springer-Verlag, Berlin, pp. 89–119.

Inoue, S., Fujihara, S., 2010. Synthesis of inorganic–organic layered compounds using immiscible liquid–liquid systems under the distribution law. Langmuir 26, 15938–15944. http://dx.doi.org/10.1021/la1028542.

Jobbágy, M., Regazzoni, A.E., 2011. Dissolution of nano-size Mg–Al–Cl hydrotalcite in aqueous media. Appl. Clay Sci. 51, 366–369. http://dx.doi.org/10.1016/j.clay.2010.11.027.

Kongshaug, K.O., Fjellvåg, H., 2004. Organically pillared layered zinc hydroxides. J. Solid State Chem. 177, 1852–1857. http://dx.doi.org/10.1016/j.jssc.2004.01.017.

Meyn, M., Beneke, K., Lagaly, C., Chemie, A., Kiel, U., 1993. Anion-Exchange Reactions of Hydroxy Double Salts. pp. 1209–1215.

Miao, J., Xue, M., Itoh, H., Feng, Q., 2006. Hydrothermal synthesis of layered hydroxide zinc benzoate compounds and their exfoliation reactions. J. Mater. Chem. 16, 474. http://dx.doi.org/10.1039/b511110b.

Mohanambe, L., Vasudevan, S., 2005. Anionic clays containing anti-inflammatory drug molecules: comparison of molecular dynamics simulation and measurements. J. Phys. Chem. B 109, 15651–15658. http://dx.doi.org/10.1021/jp050480m.

Nakamoto, K., 1997. Infrared and Raman Spectra of Inorganic and Coordination Compounds. 5th ed. Wiley and Sons, New York.

Parello, M.L., Rojas, R., Giacomelli, C.E., 2010. Dissolution kinetics and mechanism of Mg–Al layered double hydroxides: a simple approach to describe drug release in acid media. J. Colloid Interface Sci. 351, 134–139. http://dx.doi.org/10.1016/j.jcis.2010.07.053.

Poul, L., Jouini, N., Fie, F., 2000. Layered Hydroxide Metal Acetates (Metal) Zinc, Cobalt, and Nickel): Elaboration via Hydrolysis in Polyol Medium and Comparative Study. pp. 3123–3132.

Richardson-Chong, S.S.D., Patel, R., Williams, G.R., 2012. Intercalation and controlled release of bioactive ions using a hydroxy double salt. Ind. Eng. Chem. Res. 51, 2913–2921. http://dx.doi.org/10.1021/ie202036y.

Rives, V., Del Arco, M., Martín, C., 2013. Layered double hydroxides as drug carriers and for controlled release of non-steroidal antiinflammatory drugs (NSAIDs): a review. J. Control. Release 169, 28–39. http://dx.doi.org/10.1016/j.jconrel.2013.03.034.

Rives, V., del Arco, M., Martín, C., 2014. Intercalation of drugs in layered double hydroxides and their controlled release: a review. Appl. Clay Sci. 88–89, 239–269. http://dx.doi.org/10.1016/j.clay.2013.12.002.

Rodrigues, L.A.D.S., Figueiras, A., Veiga, F., de Freitas, R.M., Nunes, L.C.C., da Silva Filho, E.C., da Silva Leite, C.M., 2013. The systems containing clays and clay minerals from modified drug release: a review. Colloids Surf. B Biointerfaces 103, 642–651. http://dx.doi.org/10.1016/j.colsurfb.2012.10.068.

Rojas, R., 2014. Copper, lead and cadmium removal by Ca Al layered double hydroxides. Appl. Clay Sci. 87, 254–259. http://dx.doi.org/10.1016/j.clay.2013.11.015.

Rojas, R., Giacomelli, C.E., 2013. Effect of structure and bonding on the interfacial properties and the reactivity of layered double hydroxides and Zn hydroxide salts. Colloids Surf. A Physicochem. Eng. Asp. 419, 166–173. http://dx.doi.org/10.1016/j.colsurfa.2012.12.002.

Rojas, R., Barriga, C., De Pauli, C.P., Avena, M.J., 2010. Influence of carbonate intercalation in the surface-charging behavior of Zn–Cr layered double hydroxides. Mater. Chem. Phys. 119, 303–308. http://dx.doi.org/10.1016/j.matchemphys.2009.09.001.

Rojas, R., Palena, M.C., Jimenez-Kairuz, A.F., Manzo, R.H., Giacomelli, C.E., 2012. Modeling drug release from a layered double hydroxide–ibuprofen complex. Appl. Clay Sci. 62–63, 15–20. http://dx.doi.org/10.1016/j.clay.2012.04.004.

Rojas, R., Jimenez-Kairuz, A.F., Manzo, R.H., Giacomelli, C.E., 2014. Release kinetics from LDH-drug hybrids: effect of layers stacking and drug solubility and polarity. Colloids Surf. A Physicochem. Eng. Asp. 463, 37–43. http://dx.doi.org/10.1016/j.colsurfa.2014.09.031.

San Román, M.S., Holgado, M.J., Salinas, B., Rives, V., 2012. Characterisation of diclofenac, ketoprofen or chloramphenicol succinate encapsulated in layered double hydroxides with the hydrotalcite-type structure. Appl. Clay Sci. 55, 158–163. http://dx.doi.org/10.1016/j.clay.2011.11.010.

Taj, S.F., Singer, R., Nazir, T., Williams, G.R., 2013. The first hydroxy double salt tablet formulation. RSC Adv. 3, 358. http://dx.doi.org/10.1039/c2ra21339g.

Williams, G.R., Crowder, J., Burley, J.C., Fogg, A.M., 2012. The selective intercalation of organic carboxylates and sulfonates into hydroxy double salts. J. Mater. Chem. 22, 13600. http://dx.doi.org/10.1039/c2jm32257a.

Wypych, F., Arízaga, G.G.C., da Costa Gardolinski, J.E.F., 2005. Intercalation and functionalization of zinc hydroxide nitrate with mono- and dicarboxylic acids. J. Colloid Interface Sci. 283, 130–138. http://dx.doi.org/10.1016/j.jcis.2004.08.125.

Yang, J., Han, Y., Park, M., Park, T., Hwang, S., Choy, J., 2007. New inorganic-based drug delivery system of indole-3-acetic acid-layered metal hydroxide nanohybrids with controlled release rate. pp. 2679–2685.

Zhang, Y., Evans, J.R.G., 2012. Alignment of layered double hydroxide platelets. Colloids Surf. A Physicochem. Eng. Asp. 408, 71–78. http://dx.doi.org/10.1016/j.colsurfa.2012.05.033.

Please cite this article as: Rojas, R., et al., Structural and physicochemical aspects of drug release from layered double hydroxides and layered hydroxide salts, Appl. Clay Sci. (2015), http://dx.doi.org/10.1016/j.clay.2015.02.030